Intergenic suppression of the γM23K uncoupling mutation in F_0F_1 ATP synthase by βGlu-381 substitutions: the role of the β^{380}DELSEED^{386} segment in energy coupling

Christian J. KETCHUM, Marwan K. AL-SHAWI and Robert K. NAKAMOTO[1]

Department of Molecular Physiology and Biological Physics, University of Virginia, P.O. Box 10011, Charlottesville, VA 22906-0011, U.S.A.

We previously demonstrated that the *Escherichia coli* F_0F_1-ATP synthase mutation, γM23K, caused increased energy of interaction between γ- and β-subunits which was correlated to inefficient coupling between catalysis and transport [Al-Shawi, Ketchum and Nakamoto (1997) J. Biol. Chem. **272**, 2300–2306]. Based on these results and the X-ray crystallographic structure of bovine F_1-ATPase [Abrahams, Leslie, Lutter and Walker (1994) Nature (London) **370**, 621–628] γM23K is believed to form an ionized hydrogen bond with βGlu-381 in the conserved β^{380}DELSEED^{386} segment. In this report, we further test the role of γ–β-subunit interactions by introducing a series of substitutions for βGlu-381 and γArg-242, the residue which forms a hydrogen bond with βGlu-381 in the wild-type enzyme. βE381A, D, and Q were able to restore efficient coupling when co-expressed with γM23K. All three mutations reversed the increased transition state thermodynamic parameters for steady state ATP hydrolysis caused by γM23K. βE381K by itself caused inefficient coupling, but opposite from the effect of γM23K, the transition state thermodynamic parameters were lower than wild-type. These results suggest that the βE381K mutation perturbs the γ–β-subunit interaction and the local conformation of the β^{380}DELSEED^{386} segment in a specific way that disrupts the communication of coupling information between transport and catalysis. βE381A, L, K, and R, and γR242L and E mutations perturbed enzyme assembly and stability to varying degrees. These results provide functional evidence that the β^{380}DELSEED^{386} segment and its interactions with the γ-subunit are involved in the mechanism of coupling.

INTRODUCTION

The multi-subunit F_0F_1-ATP synthase couples energy from transport of protons down their electrochemical gradient to synthesis of ATP (for reviews, see [1–7]). In the complex from *Escherichia coli*, the membranous F_0 sector, made up of one *a*-subunit, two *b*-subunits and approximately 12 *c*-subunits, carries out proton transport [8,9], while the soluble F_1 sector, made up of five different subunits, three α, three β, and a single copy each of γ, δ, and ε, contains the three catalytic sites. The X-ray crystallographic structure of the bovine F_1 sector [10] showed that the α- and β-subunits alternate in a hexameric ring and surround a coiled-coil of the γ-subunit terminal helices. Taking advantage of this structural information, several laboratories [11–13] demonstrated that γ rotates relative to the α–β hexamer as a part of a cooperative catalytic mechanism. Without question, the rotation is also responsible for the transmission of coupling information from the transport mechanism in the F_0 sector. Genetic and chemical cross-linking studies have accumulated evidence that inter-subunit interactions involving γ-, ε- and *c*-subunits, all of which probably rotate as a unit, play critical roles in coupling (see [14–16] for discussion).

The concerted rotation of a group of subunits relative to others must involve specific transient intersubunit interactions that are critical for the transmission of energy. In this regard, we have carefully characterized the effects of one particular mutation, γMet-23 replaced with Lys, which caused a perturbation in energy coupling between transport and catalysis [17]. Analysis of the X-ray crystallographic structure of F_1 [10] suggested that the ε-amino group of γLys-23 is in a position to form an ionized hydrogen bond with the carboxylic acid of βGlu-381 (see Figure 1, positions of residues are from the coordinates of Abrahams et al. [10]). Evidence from Arrhenius analysis of steady state ATPase activity established that the additional interaction was indeed plausible. Increased enthalpic and entropic transition state parameters indicated that additional bonds needed to be broken between the enzyme and substrate or within the enzyme to achieve the transition state in the γM23K enzyme, clearly consistent with the formation of an additional hydrogen bond between γM23K and βGlu-381 [18]. The second-site mutation, γQ269R, which according to the crystallographic structure is distant from γM23K but is also in the γ–β interface, reduced the increased thermodynamic transition state parameters and restored efficient coupling to the γM23K enzyme. We postulated that the γQ269R mutation as well as several other second-site suppressors of γM23K found among residues γ269–280 [19] counteracted the inefficient coupling effect of γM23K by reducing the energy of interaction between γ- and β-subunits [18]. Another second-site mutation that suppresses the growth defect of γM23K was γR242C [19], a residue which forms an ionized hydrogen bond with one of the βGlu-381 residues in the X-ray crystallographic structure [10]. From kinetic analysis of unisite catalysis [20] and steady state analysis of ATP synthesis [15], we found evidence indicating that the γM23K mutation disrupts the utilization of binding energy to promote catalysis and creates a branched pathway that bypassed the kinetic step that coincides with the input of $\Delta\mu_{H^+}$ energy from the F_0 sector. Based on these results, we have proposed that the additional γ–β-subunit interaction directly perturbs the transmission of coupling information between transport and catalysis [15].

In light of the above results, the rotation of the γ-subunit as a part of the catalytic cycle, and the absolute conservation of

[1] To whom correspondence should be addressed.

γMet-23, βGlu-381 and γArg-242, the question arises as to whether restoration of efficient coupling was only by modulation of general γ–β interactions, or if there were also specific structural interactions between γ-subunit residues and βGlu-381, and conformational restraints of the β^{380}DELSEED^{386} segment, that were required for efficient coupling and catalytic turnover. Previous reports have implicated βGlu-381 and other residues in the highly conserved β^{380}DELSEED^{386} segment to have a role in catalysis. For example, modification of one of the carboxylic acids by quinacrine mustard inactivated the enzyme [21]. $CuCl_2$-induced disulphide bond formation between βE381C and εS108C or γCys-87 also inactivated the enzyme and did so in a manner that was sensitive to the presence of MgADP or MgATP (or AMPPNP [22,23]. Furthermore, Duncan et al. [11] found that a disulphide bond between βE380C or one β-subunit and γCys-87 was switched to one of the other βE380C residues when MgATP was added after reduction of the disulphide.

To address the above question, we have replaced βGlu-381 and γArg-242 with a number of site-directed mutations allowing us to directly evaluate the role of these residues. Of these mutations, βE381A, D and Q reversed the effects of γM23K demonstrating the functional interaction between these residues. Furthermore, βE381K alone caused inefficient coupling. Unlike the effects of γM23K, however, βE381K appeared to cause a localized structural perturbation that disrupted proper communication of coupling information.

EXPERIMENTAL

Strains and plasmids

The *unc* operon-deleted *E. coli* stain, DK8 (*bglR*, *thi-1*, *rel-1*, *HfrPO1*, Δ(*uncB-uncC*) *ilv::Tn10*), was described previously [24]. The expression plasmid pBWU13.4, which carries the eight structural genes for the F_0F_1 complex, was derived from the previously described pBWU13 [25]. It includes a *Spe*I restriction site between *uncG* and *D* introduced by site-directed mutagenesis [26] and a *Kpn*I site between *uncA* and *G* (see below). pUβSE was derived from pUC18 and contains a portion of *uncD* (β-subunit gene) between *Sac*I and *Eco*47III. pBγKS was derived from pBluescript II KS$^-$ (Stratagene) and contains the entire *uncG* (γ-subunit gene) between *Kpn*I and *Spe*I.

Molecular biology procedures

Molecular biology procedures were performed according to manufacturers' instructions or as detailed by Sambrook et al. [27]. Restriction and DNA-modifying enzymes were obtained from Amersham Inc., Boehringer–Mannheim, Gibco–BRL, New England Biolabs, and Promega. A Stratagene Chameleon kit was used for oligonucleotide-directed mutagenesis [28]. Oligonucleotides were synthesized by Oligos Etc. (Wilsonville, OR) and are listed in Table 1. A unique *Kpn*I restriction site, 36 bp upstream of the *uncG* initiation codon, was introduced using the synthetic oligonucleotide 5′-CGTCTGGCGGgTacCCTTAGGGCAGG-CCGCA-3′ (lower case letters denote mutant bases) on a subclone between the *Asu*II site in *uncA* and *Rsr*II site in *uncG*. βGlu-381 mutations were introduced on plasmid pUβSE, isolated on *Eag*I to *Eco*47III restriction fragments and ligated into pBWU13.4. Similarly, γMet-23 and γArg-242 mutations were introduced on plasmid pBγKS then transferred to pBWU13.4 as *Kpn*I to *Spe*I cassettes. The introduction of each mutation and the absence of any other changes were confirmed by DNA sequencing [29] and phenotype.

Table 1 Synthetic oligonucleotides for site-directed mutagenesis

Mutation	Oligonucleotide sequence*
βE381A	5′-TGGGTATGGATgcgCTGTCTGAAGA-3′
βE381D	5′-TGGGTATGGATgatCTGTCTGAAGA-3′
βE381K	5′-TGGGTATGGATaaaCTGTCTGAAGA-3′
βE381L	5′-TGGGTATGGATctgCTGTCTGAAGA-3′
βE381Q	5′-TGGGTATGGATcagCTGTCTGAAGA-3′
βE381R	5′-TGGGTATGGATcgtCTGTCTGAAGA-3′
γM23K	5′-CACTAAACGCaaaGAGATGGTCGCC-3′
γR242E	5′-AGCAGGCCGCGgaaATGGTGGCGATGAA-3′
γR242L	5′-AGCAGGCCGCGctgATGGTGGCGATGAA-3′

* Lower case letters denote the mutant codon.

Growth of strains and membrane preparations

Strain DK8 harbouring derivatives of pBWU13.4 were grown on supplemented minimal medium as previously described [25,30]. For determination of oxidative phosphorylation dependent growth, 0.4 % sodium succinate was used as the sole carbon source [30]. When F_0F_1-containing membrane vesicles were to be prepared, strains were grown until mid log in minimal medium containing 1.1 % glucose at 37 °C. Membranes were isolated as previously described [31]. Protein concentrations were determined by the method of Lowry et al. [32]. Membrane preparations were made from each mutant strain twice and all assays were performed at least twice on each preparation. Reported values are the averages of all repetitions ± S.D.

Determination of F_1 content

Determination of F_1 content in membrane preparations was performed by a quantitative immunoblot analysis described previously [18]. Purified F_1 [33] was used as a reference standard.

Enzymic assays

Formation of an electrochemical gradient of protons assayed by Acridine Orange fluorescence quenching and ATP hydrolysis rates were measured in conditions as previously described [18,34]. Inhibition of ATPase activity by aurovertin D was determined at a concentration of 10 μM. For Arrhenius analysis, temperature dependence of ATPase activity was measured in buffers with the pH adjusted at the appropriate temperature [18]. The concentration of free Mg^{2+} and MgATP was calculated using the algorithm of Fabiato and Fabiato [35].

RESULTS

Properties of the γM23K mutant enzyme in the DK8/pBWU13 system

Expression of the F_0F_1 complex in the DK8/pBWU13 system resulted in approx. 10- to 20-fold higher levels of the enzyme than those obtained from the native chromosomal-encoded *unc* operon [25]. We accurately determined the content of F_1 in this system (pBWU13.4 is a slightly modified version of pBWU13, see Experimental section) using a quantitative immunoblot

Table 2 Effect of βGlu-381 and γArg-242 mutations with co-expression of γM23K*

Strain *DK8/pBWU13.4*	F_1 content of membrane preparations† (range % of total protein)	Turnover of ATP hydrolysis at 25 °C‡ (% of WT)	ATP-dependent H^+ pumping at 25 °C (% of WT)
Wild-type	18–24	100 ± 0	100 ± 0
pBR322	0	0 ± 0	0 ± 0
γM23K	8–10	29 ± 2	10 ± 2
βE381D	14–20	90 ± 1	98 ± 1
βE381D + γM23K	12–17	35 ± 2	84 ± 1
βE381Q	12–18	85 ± 1	97 ± 1
βE381Q + γM23K	13–17	36 ± 2	66 ± 2
βE381A	2–3	108 ± 6	25 ± 2
βE381A + γM23K	8–11	31 ± 2	55 ± 4
βE381L	14–19	44 ± 1	96 ± 1
βE381L + γM23K	16–25	11 ± 1	1 ± 0
βE381K	1–9	90 ± 9	0 ± 0
βE381K + γM23K	11–15	22 ± 1	8 ± 1
βE381R	12–15	50 ± 1	88 ± 2
βE381R + γM23K	0	N.D.	N.D.
γR242L	8–9	70 ± 2	88 ± 3
γR242L + γM23K	18–24	21 ± 1	0 ± 0
γR242L + βE381R	8–13	36 ± 3	0 ± 0
γR242E	0	N.D.	N.D.
γR242E + γM23K	0	N.D.	N.D.
γR242E + βE381R	0	N.D.	N.D.

* See Experimental section for assay conditions.

† Range of F_1 associated with membrane preparations expressed as percent of total membrane protein.

‡ Turnover number for the membranous wild-type F_0F_1 enzyme was 260 ± 5/s (mean ± S.D. from six experiments.) Turnover numbers were derived by dividing the ATPase activity by the experimentally determined concentration of F_1 in the membranes. See Experimental section for details.

N.D., not done.

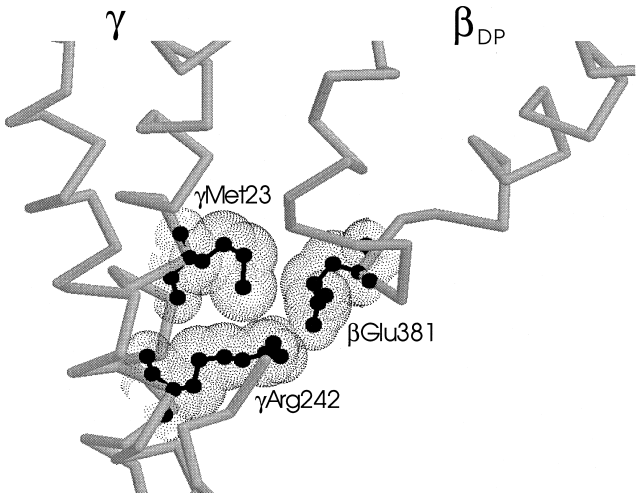

Figure 1 Spatial relationship among βGlu-381, γMet-23 and γArg-242 based on the X-ray crystallographic model of Abrahams et al. [10]

The βDELSEED segment from β_{DP} is on the right and the γ helices are on the left.

system [18] and found that F_1 constituted approximately 20 %, and therefore F_0F_1 28 %, of inner membrane protein (Table 2). Despite the overexpression, turnover numbers for ATP hydrolysis were very similar to those obtained with the lower expressing KF10rA/pBWG15 system [18].

We previously reported that the γM23K mutant F_0F_1 expressed in strain KF10rA/pBMG15 was not able to support oxidative phosphorylation-dependent growth; however, there was a reproducibly small amount of growth in liquid culture with succinate as the sole carbon source (5 % of wild-type [17]). This result indicated that the γM23K was capable of net ATP synthesis despite its uncoupling phenotype. This behaviour was confirmed by measurement of NADH-driven ATP synthesis *in vitro* [18]. We expected that overexpression of the mutant protein would result in increased total levels of ATP synthesis and growth on succinate. In liquid cultures where oxidative phosphorylation-dependent growth was determined using succinate as the sole carbon source, the DK8/pBWU13.4-γM23K strain grew to 62 % of wild-type at 37 °C (data not shown).

βE381D, Q and A restored efficient coupling to the γM23K mutant enzyme

As discussed in the Introduction, the effect on coupling by the γM23K mutation and the interactions between this residue and βGlu-381 led us to predict that changes of βGlu-381 would affect coupling as well. Table 2 indicates the ATP-dependent H^+ pumping of various βGlu-381 mutant enzymes. As single mutations, the relatively conservative substitutions of Asp or Gln replaced the wild-type Glu with only minor effects. In contrast, the βE381A mutation caused a decreased level of ATP-dependent H^+ pumping to 25 % of wild-type (Table 2). Additionally, the βE381A mutation decreased the efficiency of complex assembly (12 % of wild-type F_1 on the membranes expressed in the DK8/pBWU13.4 system). Nevertheless, the mutant F_1 complex appeared to be bound to F_0 in a stable manner as the membranes were still able to generate a normal NADH-driven electrochemical gradient of protons. This result was an indication that the membranes did not have a passive leak of protons due to F_0 left unoccupied because of dissociated mutant F_1 (data not shown). Furthermore, the hydrolytic turnover number of the βE381A mutant enzyme was similar to wild-type indicating that the mutation did not cause a gross misfolding of the β-subunits (see below).

Most importantly, all three of these mutations, βE381D, Q and A, resulted in F_0F_1 complexes with increased coupling efficiency in the γM23K enzyme. The return of coupling function is demonstrated by the H^+ pumping experiments shown in Figure 2. Co-expression of βE381D, Q or A with γM23K restored ATP-dependent H^+ pumping to 83, 66 or 55 % of wild-type, respectively, compared with 10 % for γM23K alone. In control experiments, normal NADH-driven electrochemical gradients of protons were generated in the mutant membranes demonstrating that there was no excessive leak of protons (data not shown). In the case of βE381A, the two mutations mutually suppressed each other as the γM23K/βE381A double mutant had more enzyme complex in the membranes and more ATP-driven H^+ pumping (Table 2) indicating that βE381A was stabilized by γM23K. These results implicated βGlu-381 and the β^{380}DELSEED^{386} segment in the coupling mechanism.

βE381K mutation causes inefficient coupling

Like the βE381A mutation, changes to the larger neutral Leu or positively charged Arg and Lys perturbed assembly of the complex as denoted by the lower levels of enzyme on the membranes (Table 2). In addition and most significantly, the βE381K mutant enzyme had no ATP-dependent H^+

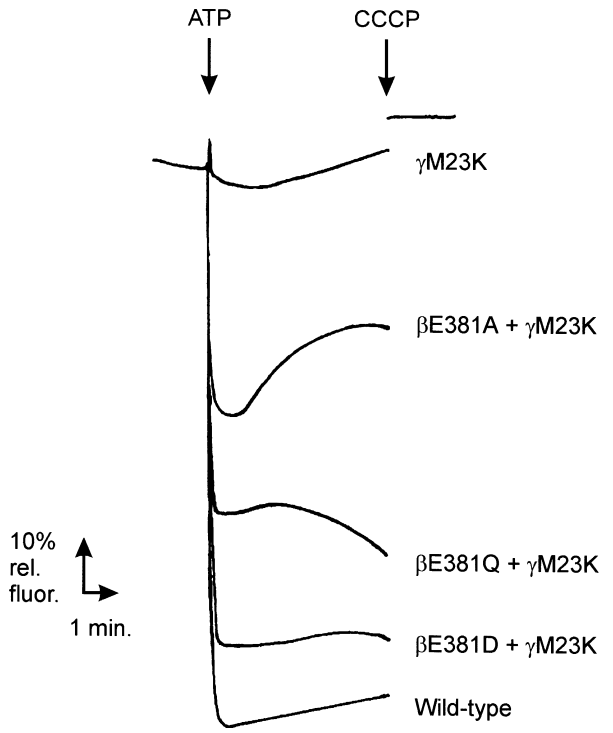

Figure 2 Formation of an electrochemical gradient of protons by γM23K/β381 mutant enzymes

Acridine Orange fluorescence quenching was monitored at 530 nm with excitation at 460 nm. 100 μg of membrane vesicle protein was suspended in 1 ml of a buffer containing 10 mM Hepes-KOH, 300 mM KCl, 5 mM $MgCl_2$, 1 μM valinomycin, and 1 μM Acridine Orange at pH 7.5, 25 °C, with vigorous mixing. Proton pumping was started with the addition of 1 mM ATP. 1 μM carbonylcyanide-*m*-chlorophenylhydrazone (CCCP) was added to end the reaction and to establish the 100% fluorescence value.

pumping activity despite a hydrolytic turnover number that was 87% of wild-type and no passive leak of protons. The level of mutant enzyme on the membranes was greatly reduced; however, other enzymes with less F_0F_1 complex in the membrane were still able to generate sizable electrochemical gradients of protons (e.g. βE381A or wild-type in the KF10rA/pBWG15 system, [18]). The βE381K mutant strain also did not grow under oxidative phosphorylation-dependent conditions when succinate was used as the sole carbon source (0% of wild-type at 37 °C). Clearly, the βE381K mutation caused inefficient coupling. Interestingly, the βE381R enzyme appeared to have relatively normal coupling (Table 2). Unlike the βE381A mutation, βE381L, K or R were unable to restore oxidative phosphorylation-dependent growth or ATP-dependent H^+ pumping to the γM23K mutant enzyme. βE381L and K repaired the ability of γM23K to assemble to some extent, but the double mutants, βE381L or K/γM23K, had very low catalytic turnover and ATP-dependent H^+ pumping (Table 2). In contrast, the βE381R/γM23K double mutant complex did not assemble.

As discussed in the Introduction, the X-ray crystallographic F_1 structure [10] suggested that γArg-242 interacts with both βGlu-381 and γMet-23 (Figure 1). In addition, we previously reported that the γR242C mutation genetically suppressed γM23K [19] not because the cysteine replacement increased coupling efficiency, but because γR242C caused an increased turnover rate which compensated for the inefficient coupling [18]. Consequently, we expected that replacements of this residue would also influence function. We report here that replacement with Leu perturbed assembly of the complex, and did not improve coupling efficiency of the γM23K enzyme (Table 2). Replacement of γArg-242 by Glu proved even more drastic as the acidic residue resulted in no detectable F_1 complex in membrane preparations. This effect was similar to the disruptive effect of placing an amino acid of opposite charge in place of βGlu-381 (see above), and might be interpreted as repulsion between residues of the same charge on γ- and β-subunits that caused destabilization of the F_1 complex. However, simply switching the positions of the two charged residues to make the γR242E/βE381R double mutant did not create a functional complex as no F_1 complex was detected (Table 2). Taken together, these results suggest that the position of the charged functional groups is more important to complex assembly and stability than the charged residues themselves.

We note that none of these mutations significantly altered ATPase inhibition by aurovertin D (data not shown). Aurovertin D is an inhibitor whose binding site is physically located between the nucleotide binding site and the β^{380}DELSEED^{386} loop [36,37]. These data indicate that any conformational perturbations the mutations may have caused were localized and did not grossly alter folding of the β-subunits.

Effects of βGlu-381 replacements on transition state thermodynamic parameters

Previously, we showed a correlation between the reduced coupling efficiency of the γM23K enzyme with an increase in the transition state thermodynamic parameters of steady state hydrolysis and interpreted this as an increase in the energy of interaction between γ- and β-subunits [18]. The hypothesis was strengthened when we found that γQ269R, a second-site suppressor mutation of γM23K, restored efficient coupling and greatly reduced the differences in the transition state parameters. We suspected that replacement of βGlu-381 would have similar effects. Arrhenius analysis of steady state ATPase activities were performed in the presence of saturating substrate, an ATP regenerating system and carbonylcyanide-*m*-chlorophenylhydrazone, a protonophore, to prevent back inhibition from build up of ADP or a $\Delta\mu_{H^+}$. From these data, transition state thermodynamics parameters were derived (Table 3, [18]). Indeed, the three βGlu-381 mutations that were found to restore coupling to the γM23K enzyme, βE381A, D or Q (Table 2), reduced both enthalpic and entropic parameters of the transitions state to values closer to wild-type (Table 3). In contrast, βE381L and γR242L, which did not restore efficient coupling, did relatively little to reduce the increased transition state parameters.

The transition state thermodynamic parameters also indicated that the βE381K mutation perturbed coupling by a different mechanism. The βE381K enzyme had the opposite effect on transition state thermodynamic parameters than did γM23K (Table 3). The decreased transition state enthalpy and entropy suggested that the Lys replacement of βGlu-381 perturbed γ- and β-subunit interactions. However, because the βE381K mutant enzyme did not pump protons, it is likely that the mutation had a further effect which we propose to be a disrupted conformation of the β^{380}DELSEED^{386} segment. This additional effect of the mutation was further emphasized by the ability of the βE381K mutation to reduce the enthalpic and entropic parameters of the γM23K mutant; however, it did so without restoring efficient coupling (Table 2). The βE381K mutation appears to have reduced the energy of interaction between the γM23K γ-subunit and β-subunits but did not allow more efficient

Table 3 Transition state thermodynamic parameters ± standard deviation of the steady state ATP hydrolysis reaction at 25 °C for membranous F_0F_1

Values for $\Delta H^{\ddagger}$ and $T\Delta S^{\ddagger}$ were determined from combined Arrhenius analysis data. Values for $\Delta G^{\ddagger}$ were derived from turnover determinations at 25 °C. $\Delta\Delta$ values are differences between parameters for mutant enzyme and the corresponding wild-type.

Strain	$\Delta H^{\ddagger}$ (kJ/mol)	$T\Delta S^{\ddagger}$ (kJ/mol)	$\Delta G^{\ddagger}$ (kJ/mol)
WT	44.0 ± 0.5	−15.2 ± 0.5	59.2 ± 0.05
	$\Delta(\Delta H^{\ddagger})$	$\Delta(T\Delta S^{\ddagger})$	$\Delta(\Delta G^{\ddagger})$
γM23K	26.3 ± 1.2	23.2 ± 1.1	3.1 ± 0.2
βE381D	−3.1 ± 0.6	−3.4 ± 0.6	0.3 ± 0.0
βE381D + γM23K	8.6 ± 1.2	5.9 ± 1.2	2.7 ± 0.1
βE381Q	1.0 ± 0.2	0.5 ± 0.2	0.4 ± 0.0
βE381Q + γM23K	5.8 ± 0.9	3.3 ± 0.9	2.6 ± 0.1
βE381A	−7.0 ± 1.1	−6.9 ± 1.0	−0.1 ± 0.1
βE381A + γM23K	4.0 ± 1.3	1.0 ± 1.2	1.2 ± 0.2
βE381K	−13.7 ± 1.7	−14.0 ± 1.7	0.3 ± 0.2
βE381K + γM23K	−5.7 ± 1.0	−9.5 ± 1.0	3.9 ± 0.1
βE381L	3.1 ± 1.3	1.0 ± 1.2	2.1 ± 0.0
βE381L + γM23K	17.7 ± 0.7	12.2 ± 0.7	5.5 ± 0.1
γR242L	0.7 ± 0.5	−0.2 ± 0.5	1.0 ± 0.1
γR242L + γM23K	32.5 ± 2.2	28.5 ± 2.1	4.0 ± 0.1

coupling because the mutation also disrupted coupling linkage by altering the conformation of the β^{380}DELSEED^{386} segment.

We point out that other mutations which decreased enthalpic and entropic parameters had impaired enzyme function without affecting coupling, most notably γQ269E, a mutation with reduced turnover number but catalytic activity that is coupled to transport ([34], and Al-Shawi, M. K. and Nakamoto, R. K., unpublished observations). The residue γGln-269 normally interacts with a β-subunit through the loop containing residue βThr-308 [10]. Hence, the observed decreases in enthalpic and entropic parameters are thought to represent reductions in the interaction energy between γ- and β-subunits [18].

DISCUSSION

As detailed in the Introduction, the β-subunit ^{380}DELSEED^{386} segment and its interactions with the γ-subunit are important in catalytic turnover. We have used mutagenic and thermodynamic analyses to establish that interactions of this conserved segment with the γ-subunit are also important in coupling between catalysis and transport. Two results led to this conclusion. First, the βE381A, D and Q mutations restored coupling efficiency to the γM23K mutant enzyme. The suppressive effect of these mutations was similar to a previously characterized intragenic second-site mutation, γQ269R [18]. All of these mutations restored efficient coupling to the γM23K mutant and reduced the transition state enthalpic and entropic parameters for steady state ATP hydrolysis of the γM23K enzyme closer to wild-type values (Table 3). These results are completely consistent with our previous analyses that demonstrated that the second site mutations restore efficient coupling by decreasing the energy of interaction between γ- and β-subunits. Based on the X-ray crystallographic structure [10], the β381 mutant amino acids do not form ionized hydrogen bonds with γM23K or γArg-242 as the wild-type Glu (see Figure 1). The carboxylic acid group of the smaller Asp is likely to have a different orientation of the carboxylic acid relative to Glu; the amino group of Gln has a different hydrogen-bond chemistry; and the side chain of βE381A does not contribute ionic interactions [38]. Second, the βE381K mutation by itself perturbed coupling efficiency. In contrast to γM23K, this mutation caused decreased transition state parameters of ATP hydrolysis relative to wild-type (Table 3). It is likely that βE381K caused an unfavourable conformational effect that blocked the communication of coupling information and disrupted the assembly and stability of the complex as indicated by the reduced amount of mutant F_1 detected on the membranes (Table 2). It is possible that the perturbation involved unfavourable interactions between residues γArg-242 and βE381K, or more likely, the local conformation of the β^{380}DELSEED^{386} segment, perhaps in the form of excess conformational flexibility. The perturbation of coupling is specific for Lys as other βGlu-381 replacements including Arg did not appear to affect coupling although many of the mutations did affect assembly and stability. At least for the mutant complexes that assembled, the conformational perturbations appeared to be localized and did not involve gross structural changes in β-subunits because aurovertin D inhibition of ATPase activity was not altered. We emphasize that the uncoupling effect of βE381K represents a different mechanism of perturbing coupling as compared with that proposed for γM23K. The γM23K mutation caused increased energy of interaction between γ- and β-subunits, whereas the βE381K mutation likely introduced an unfavourable interaction and a localized conformational perturbation. Its disruptive effect on γ–β interactions strengthens our notion that the communication of coupling information proceeds from the γ-subunit helices through the β^{380}DELSEED^{386} segments to the catalytic sites [18].

These results are relevant to 'rotational catalysis'. This model, which has been discussed extensively elsewhere [14–16], invokes rotation of at least the γ- and ϵ-subunits relative to the $\alpha_3\beta_3$ hexamer and in this manner drives the three catalytic sites sequentially through their cycles offset from each other by 120°. We have previously presented a kinetic model which explicitly indicates the steps and conformations required for energy conservation [15]. This model readily explains the characteristics of steady-state turnover and site–site cooperativity. Based on kinetic analyses, the transition state monitored by the steady state Arrhenius analysis, as done in this paper, can be assigned to the power stroke of the rotational binding-energy-change mechanism. This step is likely to involve the rotation of the γ-subunit which leads to the changes in β-subunit conformation and nucleotide affinities (see Figure 7 of [15]). Most significantly, we demonstrated by isokinetic analysis that this rate limiting step is the same for ATP hydrolysis and synthesis. As for amino acid replacements affecting γ–β subunit interactions (such as γM23K, γQ269E or R, and replacements of βGlu-381), this analysis explains the dramatic changes in transition state enthalpy and entropy while the transition state free energy remains relatively unaffected. The mutations do not affect the basic catalytic mechanism and utilize the same transition state. We point out that some mutant enzymes (e.g. βR242C [39]) do significantly alter the catalytic mechanism and also alter the transition state free energy.

As the γ-subunit rotates, a different face is presented to each of the β-subunits, and in this manner induces conformational transitions. From careful inspection of the X-ray crystallographic structure [40], one expects a complex series of subunit–subunit interactions that must take place during each revolution of the γ-subunit (as well as other interactions among other subunits). Analyses of many γ- and β-subunit mutants described previously [15,18–20,34] and in this paper suggest that there are two aspects

to these interactions: (1) There is a critical balance between the energy needed to maintain complex stability versus that needed to break bonds to achieve catalytic turnover and energy coupling. This balance was dramatically demonstrated by the suppression of γM23K by mutations in the γ-subunit carboxyl terminal region (e.g. γQ269R and γT273S) [19] and the suppression of γQ269E and γT273V by mutations close to γMet-23 and γArg-242 [34]; regions which are both part of the coiled coil formed by the γ-subunit terminal helices but are separated by greater than 40 Å. From the X-ray crystallographic structure, we find that the three regions of the γ-subunit identified by the suppressor mutagenesis are exactly the regions of contact between γ and the $\alpha_3\beta_3$ hexamer. (2) The effects of these mutations also indicate that there are specific interactions required for the precise conformational changes needed for cooperativity among the sites and for efficient coupling of the transport and catalytic mechanisms. For example, the βE381K mutation affected the steady state thermodynamic parameters differently from the γM23K mutation and as discussed above probably induced a localize conformational perturbation that disrupted the transmission of coupling information through the β^{380}DELSEED^{386} segment.

Despite the evolutionary conservation of γMet-23, γArg-242, and the ^{380}DELSEED^{386} segment, none of these amino acids has yet been found to be absolutely essential for catalysis or energy coupling [17,19,22,41,42]. Furthermore, since neither γArg-242 nor βGlu-381 is essential it follows that the ionic hydrogen bond between the two residues predicted by the structural model of Abrahams et al. [10] is also not essential for enzyme function. Despite the effects of these mutations on assembly, stability or energy coupling, none affects the basic catalytic mechanism [15].

We would like to thank Dr. Stanley Dunn for the gift of aurovertin D. This work was supported by PHS grant, GM50957 to R.K.N. and GM52502 to M.K.S. C.J.K. is a recipient of a NIH predoctoral grant HL07284.

REFERENCES

1 Penefsky, H. S. and Cross, R. L. (1991) Adv. Enzymol. **64**, 173–213
2 Capaldi, R. A., Aggeler, R., Turina, P. and Wilkens, S. (1994) Trends Biol. Sci. **19**, 284–289
3 Fillingame, R. H., Girvin, M. E. and Zhang, Y. (1995) Biochem. Soc. Trans. **23**, 760–766
4 Dunn, S. D. (1995) Nature Struct. Biol. **2**, 915–918
5 Deckers-Hebestreit, G. and Altendorf, K. (1996) Annu. Rev. Microbiol. **50**, 791–824
6 Nakamoto, R. K. (1996) J. Membr. Biol. **151**, 101–111
7 Boyer, P. D. (1997) Annu. Rev. Biochem. **66**, 717–749
8 Foster, D. L. and Fillingame, R. H. (1982) J. Biol. Chem. **257**, 2009–2015
9 Hermolin, J. and Fillingame, R. H. (1989) J. Biol. Chem. **264**, 3896–3903
10 Abrahams, J. P., Leslie, A. G. W., Lutter, R. and Walker, J. E. (1994) Nature (London) **370**, 621–628
11 Duncan, T. M., Bulygin, V. V., Zhou, Y., Hutcheon, M. L. and Cross, R. L. (1995) Proc. Natl. Acad. Sci. U.S.A. **92**, 10964–10968
12 Sabbert, D., Engelbrecht, S. and Junge, W. (1996) Nature (London) **381**, 623–625
13 Noji, H., Yasuda, R., Yoshida, M. and Kinosita, K. (1997) Nature (London) **386**, 299–302
14 Cross, R. L. and Duncan, T. M. (1996) J. Bioenerg. Biomembr. **28**, 403–408
15 Al-Shawi, M. K., Ketchum, C. J. and Nakamoto, R. K. (1997) Biochemistry **36**, 12961–12969
16 Aggeler, R., Ogilvie, I. and Capaldi, R. A. (1997) J. Biol. Chem. **272**, 19621–19624
17 Shin, K., Nakamoto, R. K., Maeda, M. and Futai, M. (1992) J. Biol. Chem. **267**, 20835–20839
18 Al-Shawi, M. K., Ketchum, C. J. and Nakamoto, R. K. (1997) J. Biol. Chem. **272**, 2300–2306
19 Nakamoto, R. K., Maeda, M. and Futai, M. (1993) J. Biol. Chem. **268**, 867–872
20 Al-Shawi, M. K. and Nakamoto, R. K. (1997) Biochemistry **36**, 12954–12960
21 Bullough, D. A., Ceccarelli, E. A., Verburg, J. G. and Allison, W. S. (1989) J. Biol. Chem. **264**, 9155–9163
22 Aggeler, R., Haughton, M. A. and Capaldi, R. A. (1995) J. Biol. Chem. **270**, 9185–9191
23 Grüber, G. and Capaldi, R. A. (1996) J. Biol. Chem. **271**, 32623–32628
24 Klionsky, D. J., Brusilow, W. S. A. and Simoni, R. D. (1984) J. Bacteriol. **160**, 1055–1060
25 Moriyama, Y., Iwamoto, A., Hanada, H., Maeda, M. and Futai, M. (1991) J. Biol. Chem. **266**, 22141–22146
26 Jeanteur-De Beukelaer, C., Omote, H., Iwamoto-Kihara, A., Maeda, M. and Futai, M. (1995) J. Biol. Chem. **270**, 22850–22854
27 Sambrook, J., Fritsch, E. F. and Maniatis, T. (1989) Molecular Cloning: A Laboratory Manual, 2nd edn, Cold Spring Harbor Laboratory Press, Cold Spring Harbor
28 Deng, W. P. and Nickoloff, J. A. (1992) Anal. Biochem. **200**, 81–88
29 Sanger, F., Coulson, A. R., Barrell, B. G., Smith, A. J. H. and Roe, B. A. (1980) J. Mol. Biol. **143**, 161–178
30 Takeyama, M., Ihara, K., Moriyama, Y., Noumi, T., Ida, K., Tomiyoka, N., Itai, A., Maeda, M. and Futai, M. (1990) J. Biol. Chem. **265**, 21279–21284
31 Futai, M., Sternweis, P. C. and Heppel, L. A. (1974) Proc. Natl. Acad. Sci. U.S.A. **71**, 2725–2729
32 Lowry, O. H., Rosebrough, N. J., Farr, A. C. and Randall, R. J. (1951) J. Biol. Chem. **193**, 265–275
33 Al-Shawi, M. K. and Senior, A. E. (1992) Biochemistry **31**, 878–885
34 Nakamoto, R. K., Al-Shawi, M. K. and Futai, M. (1995) J. Biol. Chem. **270**, 14042–14046
35 Fabiato, A. and Fabiato, F. (1979) J. Physiol. (Paris) **75**, 463–505
36 Lee, R. S.-F., Pagan, J., Satre, M., Vignais, P. V. and Senior, A. E. (1989) FEBS Lett. **253**, 269–272
37 van Raaij, M. J., Abrahams, J. P., Leslie, A. G. W. and Walker, J. E. (1996) Proc. Natl. Acad. Sci. U.S.A. **93**, 6913–6917
38 Kyte, J. (1995) Structure in Protein Chemistry, Garland Publishing, New York
39 Al-Shawi, M. K., Parsonage, D. and Senior, A. E. (1990) J. Biol. Chem. **265**, 4402–4410
40 Abrahams, J. P., Buchanan, S. K., van Raaij, M. J., Fearnley, I. M., Leslie, A. G. W. and Walker, J. E. (1996) Proc. Natl. Acad. Sci. U.S.A. **93**, 9420–9424
41 Duncan, T. M., Zhou, Y., Bulygin, V., Hutcheon, M. L. and Cross, R. L. (1995) Biochem. Soc. Trans. **23**, 736–741
42 Feng, Z., Aggeler, R., Haughton, M. A. and Capaldi, R. A. (1996) J. Biol. Chem. **271**, 17986–17989

Received 21 May 1997/23 October 1997; accepted 11 November 1997